Life Sciences in Space Research 8 (2016) 22–29

Contents lists available at ScienceDirect

Life Sciences in Space Research

www.elsevier.com/locate/lssr

Monte Carlo simulations for the space radiation superconducting shield project (SR2S)

M. Vuolo [a,b,*], M. Giraudo [a,b], R. Musenich [c], V. Calvelli [c], F. Ambroglini [d], W.J. Burger [d], R. Battiston [e]

[a] Thales Alenia Space Italia, Strada Antica di Collegno, 10146 Torino, Italy
[b] Politecnico di Torino, Corso Duca degli Abruzzi 24, 10129 Torino, Italy
[c] INFN-Genova, Via Dodecaneso 33, 16146 Genova, Italy
[d] INFN-Perugia, Via Pascoli, 06123 Perugia, Italy
[e] TIFPA-INFN and University of Trento, via Sommarive 14, 38123 Trento Italy

ARTICLE INFO

Article history:
Received 7 May 2015
Received in revised form 4 December 2015
Accepted 30 December 2015

Keywords:
Radiation
Superconducting shield
Monte Carlo simulations
Dose
Deep space human missions

ABSTRACT

Astronauts on deep-space long-duration missions will be exposed for long time to galactic cosmic rays (GCR) and Solar Particle Events (SPE). The exposure to space radiation could lead to both acute and late effects in the crew members and well defined countermeasures do not exist nowadays. The simplest solution given by optimized passive shielding is not able to reduce the dose deposited by GCRs below the actual dose limits, therefore other solutions, such as active shielding employing superconducting magnetic fields, are under study. In the framework of the EU FP7 SR2S Project – Space Radiation Superconducting Shield – a toroidal magnetic system based on MgB_2 superconductors has been analyzed through detailed Monte Carlo simulations using Geant4 interface GRAS. Spacecraft and magnets were modeled together with a simplified mechanical structure supporting the coils. Radiation transport through magnetic fields and materials was simulated for a deep-space mission scenario, considering for the first time the effect of secondary particles produced in the passage of space radiation through the active shielding and spacecraft structures. When modeling the structures supporting the active shielding systems and the habitat, the radiation protection efficiency of the magnetic field is severely decreasing compared to the one reported in previous studies, when only the magnetic field was modeled around the crew. This is due to the large production of secondary radiation taking place in the material surrounding the habitat.

1. Introduction

Future manned missions to Mars and lunar outposts will require the evolution of technology and quite fascinating engineering challenges. Among the technical problems to deal with, one of the most troubling is related to ionizing radiation (Durante and Cucinotta, 2011; Cucinotta, 2013; Zeitlin et al., 2013). Reducing the health risks associated with space radiation is a fundamental prerogative to allow the execution of long duration manned interplanetary missions. The solutions studied until today involve the use of passive and active shielding (ECSS E-10-04; Spillantini, 2011). The first is based on the loss of energy due to the interactions of particles with the materials. The latter exploits magnetic fields to deflect particles.

The space radiation environment to be counteracted is mainly produced by two different components: Solar Particle Events (SPE) and Galactic Cosmic Rays (GCR).

SPE are occasional events, with possible high fluence concentrated in short periods (hours or days). Due to their relative low energy particles, they can be stopped by a passive shielded shelter (Cucinotta, 2013).

On the other hand GCR are very high energy particles arriving isotropically from outside the solar system. The GCRs, if not shielded, produce the largest contribution to the total effective dose (>500 mSv/y) in a long-duration interplanetary mission and shielding from GCR is still an open challenge due to their capability to produce secondary particles when interacting with matter. For this reason other options than the passive shielding have been investigated during the years and, among those, the use of magnetic fields to deflect radiation is one of the most interesting ones.

* Corresponding author at: Politecnico di Torino, Corso Duca degli Abruzzi 24, 10129 Torino, Italy.
E-mail address: marco.vuolo@external.thalesaleniaspace.com (M. Vuolo).

http://dx.doi.org/10.1016/j.lssr.2015.12.003
2214-5524/

The use of large superconducting magnets to generate a shielding field around the spacecraft dates back to 1960 and was subsequently proposed in several configurations (Wilson et al., 1997; Braun, 1969). However, previous works considered only the ability of the magnetic field in deflecting particles neglecting in this way the outcomes of the interaction of the charged particles with the magnetic materials necessary to generate the field (Braun, 1969; Townsend et al., 1990; Hoffman et al., 2005).

This paper describes a toroidal magnetic system studied in the framework of EU FP7 SR2S Project (Space Radiation Superconducting Shielding). Monte Carlo simulations have been used to evaluate the effective shield capability considering the combined effects of the magnetic field and materials composing the magnet, the spacecrafts and a realistic supporting structure.

The aim of the work is not to provide the values cumulated by astronauts, but to compare the dose reductions with respect to free space for several realistic shielding structures.

2. Toroidal magnetic shield

2.1. Motion of charged particles in a toroidal magnetic field

An initial trade-off between different possible active shielding structures led to the adoption of a toroidal magnetic configuration (Battiston et al., 2013; Musenich et al., 2014). The toroidal field has in fact many advantages, including an isotropic protection around the habitat and a very low fringe field inside the internal module. Clearly a toroid surrounding the spacecraft leaves the endcaps of the habitat module free of the field (and therefore protection), so eventual solutions including smaller end cap toroids could be considered to shield the side of the habitat not attached to other modules. Alternatively, passive or a combination of active and passive end cap can be used. However the treatment of this issue is beyond the scope of this work.

A scheme of the basic idea behind a toroidal shield is shown in Fig. 1. In the case of a charged particle moving radially, i.e. having zero angular velocity, the motion equation in an infinite toroidal magnetic field can be analytically solved. It can also be demonstrated that a particle with zero angular speed $\dot{\theta} = 0$ is the most penetrating one and therefore, as shown in Battiston et al. (2013) the shielding power of the toroid can be written as:

$$\Xi = \int_{R_i}^{R_e} B_\vartheta dR = \frac{\mu_0 I}{2\pi} \ln \frac{R_e}{R_i} \tag{1}$$

where I is the total current flowing in the toroid, R_e the outer radius and R_i the inner radius. The shielding power can be written also as a function of the particle properties:

$$\Xi = \frac{m_0}{q} c \sqrt{\gamma^2 - 1}(1 - \sin\varphi) \tag{2}$$

where m_0, q and γ are the particle rest mass, charge and Lorentz factor respectively. φ is the angle of incidence shown in Fig. 1.

Using (2) it is straightforward to calculate the maximum kinetic energy K_η of the particle that can be deflected by the toroidal field (Hoffman et al., 2005):

$$K_\eta = -\frac{m_0 c^2}{\eta}\left(1 - \sqrt{\left(\frac{q}{m_0 c}\frac{\Xi}{(1-\sin\varphi)}\right)^2 + 1}\right) \tag{3}$$

where η is the number of nucleons, q the charge. If the angle of incidence φ is set to $-90°$ (corresponding to a direction of a particle entering perpendicularly in the magnetic field of the toroid, being the magnetic field clockwise oriented as shown in Fig. 1) the latter

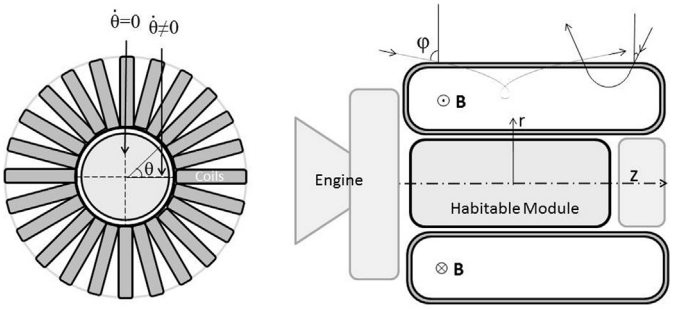

Fig. 1. Schematic view of a toroidal Space Radiation Superconducting Shield. The trajectories of two particles with different angle of incidence φ are shown.

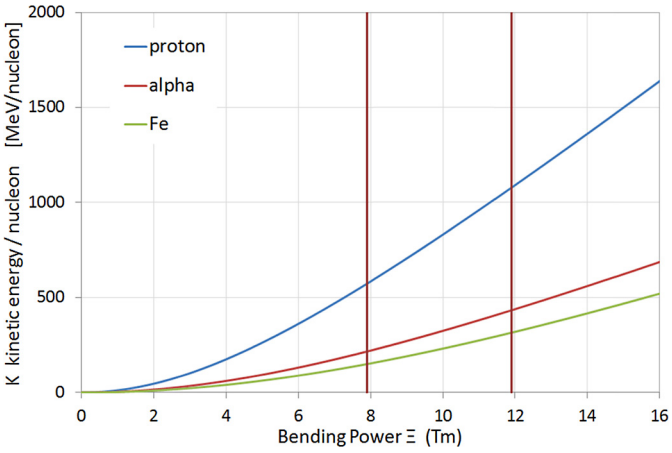

Fig. 2. Ideal "cut off" kinetic energy K_n given as a function of the bending power for protons, alpha and iron nuclei.

equation defines the shield cut-off energy. Under the previous hypothesis the ideal toroidal magnetic field with bending power Ξ is able to deflect all the particles having kinetic energy less than K_η defined in (3).

This formula can be useful to perform a first check on the magnetic field reproduced in the simulation code, while, however, the actual capability to protect the crew must be evaluated including the interaction of the cosmic rays with the materials surrounding the astronauts.

In Fig. 2 the ideal "cut off" kinetic energy K_n is given as a function of the Bending Power, for protons, He and Fe ions.

2.2. Magnet winding and mechanical structure

The SR2S superconducting magnet was thought as composed by several racetrack coils supported by a mechanical structure, whose goal is to withstand the magnetic force.

In a toroidal magnet, it is necessary to support both intra-coil forces, which tend to enlarge each coil, and the radial, inward forces resulting from the interaction of all the coils. As a consequence, the toroid needs one mechanical structure to support the intra-coil forces, and an inner one for the inward forces. In principle, under the hypothesis of perfect system symmetry, the magnet would not need any mechanical structure between the coils as no torque would be experienced by the coils. However, small mispositioning is possible in a real magnet therefore metal foam or light honeycomb will be present too to space out the coils.

Different requirements with respect to an Earth based magnet have been identified in the initial phase of the project. In particular, the mass density of the conductor and of all the materials composing the active shielding has to be minimized and the

mechanical structure should be optimized in order to reduce the whole mass; secondly the power consumption should be as low as possible compatible with an effective shielding; in addition a special attention must be paid to safety and reliability issues (e.g. it is mandatory that the active shielding system must be thermally, mechanically and electromagnetically decoupled from the habitat).

After the requirements identification, a preliminary design has been studied for the magnet and for the mechanical structures supporting it where the toroidal field is generated by a superconducting magnet wound by titanium clad, with a magnesium diboride (MgB_2) conductor with pure aluminum strip in parallel. The magnet is supposed to operate in persistent mode at 10 K, cooled by cryocoolers. A description of the magnet first design is reported in Battiston et al. (2013). Furthermore, when developing the preliminary mechanical design (not described in this work), the number of coils was raised to 120 to optimize the stress distribution.

Different choices of materials and structures have been evaluated in the first 2 years of the project, and the configurations described in the present study are based on two different concepts of mechanical structures for a 10 m long toroidal magnet for two values of shielding power: 7.9 and 11.9 Tm. These BL values resulted out of an iterative trade-off process where the main considered criteria are the following: ideal flux reduction (according to eq. (1) and at least of 90%), compatibility with the SLS Block II NASA launcher, maximum magnetic field over conductor of 4 T (according to the specification of the cable considered) and modularity (possibility to subdivide the toroid in 4 and 6 segments; Battiston et al., 2013). In particular, the simulation results reported here are referred to:

A. a first structure based on a titanium alloy coil support with tie rods made of the same material, where the inward forces are supported by an aluminum alloy cylinder (Fig. 7) (A).
B. a second one, where the coil support is made of aluminum alloy and the coil inner forces are counteracted with aramid fibers wrapped around the racetrack (Fig. 7) (B). Inward forces are supported by a cylinder made of aluminum–boron carbide cermet, a composite material capable to support very high compressive stresses. This structure is more forward-thinking than the first one, but also lighter and in principle it is composed by more effective passive shielding materials.

The mass of the systems and structures composing the configuration A is 315 tons while for the configuration B it is reduced to about 100 tons.

As regards the habitat used in our simulations, the Columbus module of the International Space Station has been chosen as a reference.

Finally, ancillary systems as the solar shield and the Meteorite and Debris Protection System (MDPS) have not been included in the simulation models because considered to have a low impact on the radiation transport through the active shielding systems.

3. Simulation models and methods

Three different sets of simulations are presented in this study. Each one was performed both with active shielding switched on, i.e. considering the magnetic field generated by the magnets, both considering the structures present in the configurations but without the magnetic field, in order to determine the relative contribution of the magnetic field to the total dose reduction.

Details on the sets of simulations will be given below.

Simulations on the different configurations were performed using the GRASv3.3 code (Geant4 Radiation Analysis in Space) (Santin et al., 2005), based on the Monte Carlo simulation toolkit Geant4.9.6 (Agostinelli et al., 2003).

Physical processes considered in this work include: ionization, bremsstrahlung, photoelectric effect, Compton scattering, elastic and inelastic hadronic interaction, nuclear capture, and particle decay. In the simulations the physics list QBBC adopted also in SPENVIS[1] was used. This list has been specifically created for radiation biology, radiation protection and space applications and it includes combinations of selected interaction models to reach higher precision in a wide energy range. In particular QBBC includes BIC (Binary Ion Cascade), BIC-Ion, BERT (Bertini), CHIPS (CHiral Invariant Phase Space), QGSP (Quark-Gluon String Precompound) and FTFP (Fritiof Precompound) models, Em opt3 was finally used as electromagnetic model (Agostinelli et al., 2003; Ivantchenko et al., 2012).

In a preliminary phase of the project the SR2S TAS-Italia simulation framework was successfully tested against literature experimental data on mono energetic proton and ion beams in different materials. Moreover, to test the magnetic field models implemented in GRAS, magnetic field values were extrapolated on a grid, matching the one obtained from the OPERA software.[2] Finally initial simulations were run to check the particles paths and the maximum kinetic energy of the deviated particles results were in agreement with the formula (3).

In the following paragraphs the definition of particle types and energies and the geometry modeling procedure will be described.

3.1. Mission scenario and environmental model

The mission scenario used as reference for this work is a deep space trip during a solar minimum, characterized by a higher flux of GCR.

Being the SPE easily shielded by both passive and active means (Durante and Cucinotta, 2011; Cucinotta, 2013), the focus of this work was on the more problematic GCR population. The model used for the description of the GCR energy spectra was the "standard ISO15390 (ECCS 10-04 standard) model at solar minimum without magnetic cut-off" (ECSS E-10-04), considering ions with atomic numbers ranging from $Z = 1$ to 26. This leads to a worst case scenario for a deep space mission. Fig. 3 shows the spectra used in the simulations for a limited subset of ions (^{1}H, ^{4}He, ^{12}C, ^{14}N, ^{16}O and ^{56}Fe) and Fig. 4 displays the relative contribution to the effective dose of each ion. These values were obtained weighting the ISO15390 GCRs fluences with the ICRP 123 "fluence to dose conversion factors" (ICRP, 2013) considering the human body in deep space without any shielding.

The reference source was modeled as a shell with radius 9.5 m. GCR protons and ions were randomly generated on its surface according to the ISO15390 spectra, and the fluence for each direction is proportional to the cosine of the angle between the source direction and the local normal to the sphere surface (cosine law with angle from 0° to 90°). These particles were then transported inside the modeled volumes.

To better characterize and compare the shielding performances it was then decided to focus the attention only on particles crossing the magnetic field, therefore, at this stage of the study, the contribution to the dose from particles coming from the EndCaps regions was not considered, being it equivalent for each configuration.

To do this, particles were generated only laterally with respect to the axial direction of the module, from a restricted area of the

[1] SPENVIS is the online ESA's Space Environment Information System: www.spenvis.oma.be.

[2] The OPERA software was used by INFN Genova to model the magnetic field, defining coils parameters (current, geometry, etc.).

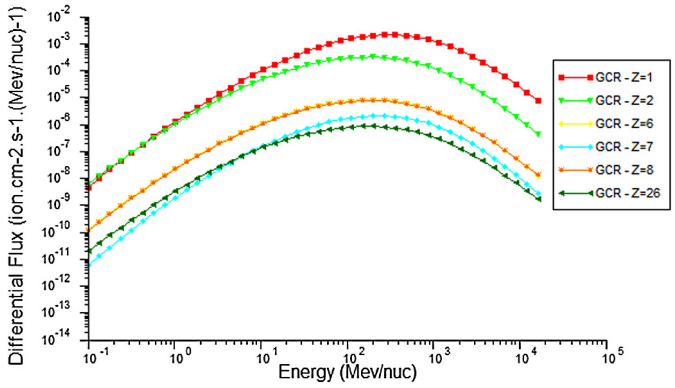

Fig. 3. Energy spectra showed for a limited subset of ions (^{1}H, ^{4}He, ^{12}C, ^{14}N, ^{16}O and ^{56}Fe) among those used in this work simulations.

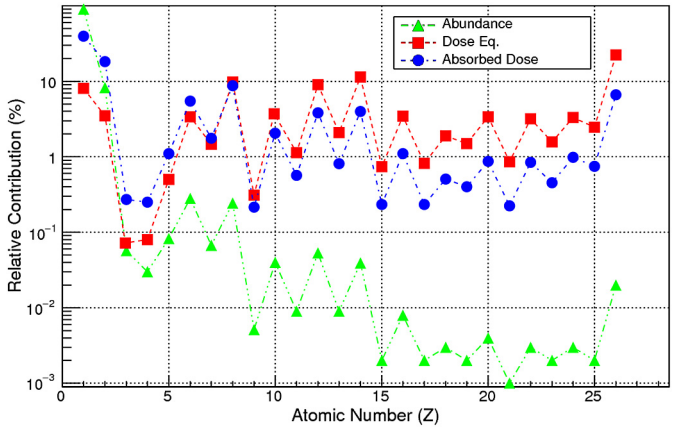

Fig. 4. Relative contribution to the absorbed dose, dose equivalent and abundance of each ion after 5 g/cm^2 of aluminum. These values have been obtained with Geant4 and are in agreement with the data reported in Durante and Cucinotta (2011).

reference spherical source, confined to a cylinder (9 m long) placed outside the region occupied by the toroid (Barrel region), as shown in Fig. 5.

3.2. Geometric model

The complete geometric model used in the simulations was built using the Geometry Description Markup Language (GDML), which allows the definition of geometry data in the XML format (Chytracek et al., 2006).

In the next sections a brief description is given for each of the modeled structures considered in this work. As already said, two different complete configurations were simulated:

A. A first one based on titanium structures to support the coils (total mass 315 tons, then parametrically varied).
B. A second one based on aramid fibers support structure reducing the total mass to 104 tons and 147 tons for a bending power of 7.9 and 11.9 Tm respectively.

The reason for which two different structures were considered is that the initial approach of the project based on the use of the most ready technology, led to the adoption of a heavy support structure mainly composed by titanium (A), but the first set of simulations revealed a too high secondary particles production, in particular high-energy neutrons. This result highlighted the necessity to use a lighter structure keeping the same bending power and therefore led to the development of the second configuration model (B), as an attempt to improve the magnetic field efficiency

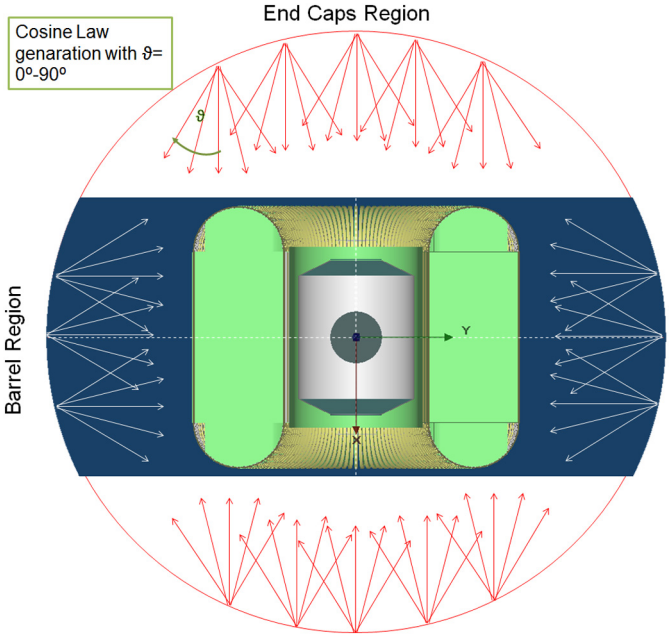

Fig. 5. SR2S reference spherical source, confined to a cylinder (9 m long) placed outside the region occupied by the toroid (Barrel region).

with the aim of making this kind of technology more attractive for future developments. Two versions of the "B" configuration were then designed (B1 and B2) in order to support two different values of bending power (7.9 Tm and 11.9 Tm). A complete geometric description of the models will be provided in the next paragraphs and their main properties can be found in Table 1.

3.2.1. Reference habitat module

As a courtesy of Thales Alenia Space Italia, it was possible to use their geometrical models of the ISS Columbus module. The structures of the magnets and of the mechanical support systems have therefore been designed to be compatible with that habitat.

3.2.2. Magnet modeling

For the configuration A, the magnet has been modeled with 120 racetrack coils made of a homogeneous material equivalent to the winding pack, composed by the conductor (Ti, Mg, B, Al), the insulation (C, O, H) and the coil support (Ti) – see Fig. 6 and Fig. 7. To improve the computational performances, the model was properly simplified: as the titanium rods are uniformly distributed within each coil, it was decided to model them as a titanium cylinder with the same mass, as shown in Fig. 7.

Configuration B1 and B2 are modeled in a more detailed way. The coil support is made of an aluminum alloy and it is considered as a different volume from the conductor and the insulation (Fig. 6, Fig. 7). The coils tie rods are replaced by an aramid fibers bandage wrapped around each racetrack structure, as shown in Fig. 7 on the right.

Configuration B2 is built keeping the same conceptual design and the same materials of configuration B1 but adapting the mass, the shape and the size of each structure to support a magnetic field with higher bending power (11.9 Tm).

The supporting structure between the coils and the habitat needed to balance the inward magnetic forces arising in the toroidal configuration (Musenich et al., 2014; Calvelli, 2013) was here modeled as a cylinder made by aluminum alloy honeycomb for configuration A and by aluminum–boron carbide cermet for configuration B1 and B2.

Table 1
Properties of the different configurations.

	Configuration A	Configuration B1	Configuration B2
Total mass	315 tons	104 tons	147 tons
Height	10 m	10 m	10 m
Winding cable material	57% Al, 9% MgB_2, 23% Ti, 11% SiO_2	57% Al, 9% MgB_2, 23% Ti, 11% SiO_2	57 %Al, 9% MgB_2, 23% Ti, 11% SiO_2
Former	Titanium	Aluminum	Aluminum
Struct. cylinder mat	Al honeycomb	B4C/Al	B4C/Al
Toroid int. radius	2.70 m	2.80 m	2.80 m
Toroid ext. radius	6.30 m	6.40 m	8.75 m
Bending power	7.9 Tm	7.9 Tm	11.9 Tm
MC simulation	Variable density: 100%, 75%, 50%, 25%, 0% Field ON and OFF	Real design density field ON and OFF	Real design density field ON and OFF

As the solar shield and the MDPS have a very low mass compared to the other structures, they were not modeled in the simulations.

Table 1 lists all the relevant data for the simulations.

3.3. Methods

In this paragraph an overview of the simulated quantities, together with the calculation hypotheses and uncertainties, is given. After that the two main categories of performed simulations are defined.

The selected quantities of interest were the dose (Gy/y) and the effective dose (Sv/y) received by the crew inside the habitat. These quantities were obtained converting fluence values registered inside the habitat into dose and effective dose using the "fluence to dose conversion factors" provided by ICRP 123 (ICRP, 2013). This procedure allows to obtain equivalent doses for each organ and tissue of the voxelized ICRP reference phantoms (male and female), computed using the ICRP and the NASA quality factors. Assuming the crew movements during the mission as uniformly distributed inside the spacecraft, it has been believed a good approximation to calculate the average fluences of primary and secondary particles entering the surface of a 2 m diameter virtual sphere placed inside the module.

The computation of particle fluences and absorbed doses in GRAS requires a normalization procedure that takes into account the particle source properties. The pursued physical quantity Q_{real} (in this case the particle fluence or the deposited dose) is obtained with Equation (4):

$$Q_{real} = F_N \cdot Q_{GRAS} \tag{4}$$

where Q_{GRAS} stands for the simulated quantity, normalized to the incident simulated event, and F_N is a normalization factor, which can be computed with Equation (5):

$$F_N = \Phi_{4\pi}\pi R^2/Np \tag{5}$$

where R is the source radius, Np the number of primary particles generated and $\Phi_{4\pi}$ is the source fluence integrated over the solid angle computed as:

$$\Phi_{4\pi}(E) = \int_0^{2\pi} d\omega \int_{-1}^{1} \Phi(E) d(\cos\vartheta) = 4\pi\Phi(E)$$

Uncertainties here considered are related only to the Monte Carlo code statistics. Epistemic uncertainties implied in the code, geometric model approximations (including compositions of materials), uncertainties in GCR fluxes (ISO 15390) (ECSS E-10-04), in the ICRP quality factors (ICRP, 2013) and in the employed physical models (ECSS E-10-04; Agostinelli et al., 2003) are not considered in this analysis. Since the goal of this work is to perform a comparison among different solutions the above-mentioned uncertainties are assumed to be the same for each case.

The relative error for each energy bin, in the fluence analysis module of GRAS, is computed during the simulations. Then errors are propagated when applying the ICRP 123 quality factors.

3.4. Configurations used in the simulations

It follows a description of the two sets of simulations presented in this work.

3.4.1. Configuration A. Parametric analysis varying the mass

The first configuration used as input was the model relative to the mechanical structure "A", having a total mass of 315 tons. The goal of this first set of simulations was to understand how the mass of the active shield, influences the effective dose on the crew inside the habitat, and so, the total shielding effectiveness. In particular, its impact on the capability to stop the incoming radiation and to generate secondary particles was evaluated varying parametrically the mass with the same geometrical model for two cases: magnetic field on and magnetic field off. For this purpose, starting from the geometric model of configuration A, the density values of coils and supporting structures materials were virtually reduced in order to decrease the total mass, leaving unchanged the designed realistic mass distribution around the crew module.

This choice is not realistic and no mechanical stress analyses were performed when varying the density, nevertheless it was very useful to understand the contribution to the total dose reduction and to the secondary particles production of the amount of materials placed around the habitat.

The following relative densities were taken into consideration, as a percentage of the real one:

- 0% of the total, with only the crew module modeled
- 25% of the total and the crew module modeled
- 50% of the total and the crew module modeled
- 75% of the total and the crew module modeled
- 100% of the total and the crew module modeled

3.4.2. Configuration B. Simulation of the mass optimized configuration

This second set of simulations was performed using as geometrical input the model relative to the mechanical structures B1 and B2. When designing these configurations the challenge was to minimize the production of high energy neutrons which have a great impact on the dose with their neutral charge allowing them not to suffer the effect of the Lorentz force inside the magnetic field.

In a first part of the work (B1) a toroidal field with bending power of 7.9 Tm, equal to the one used in the configuration A simulations, was used, then increased to 11.9 Tm (B2) to study how a relevant growth of this parameter affects the radiation transport.

Source dimensions, normalization factors and other parameters are the same as those used in the simulations described previously.

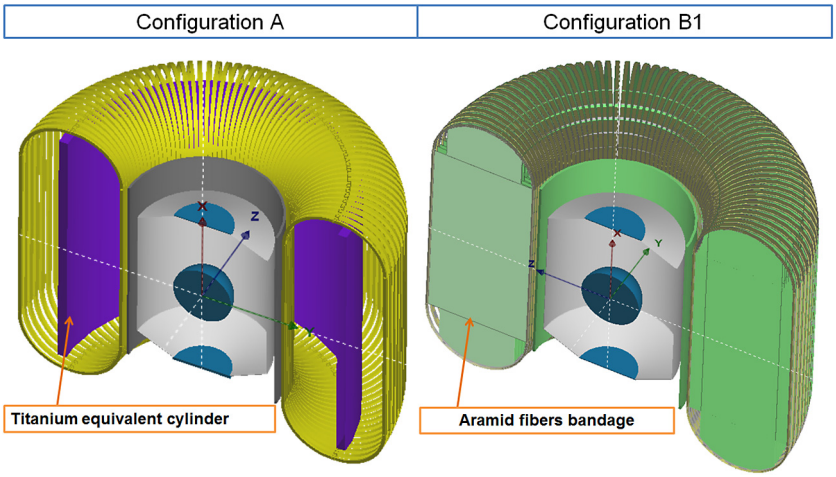

Fig. 6. SR2S geometrical models for configurations A and B1.

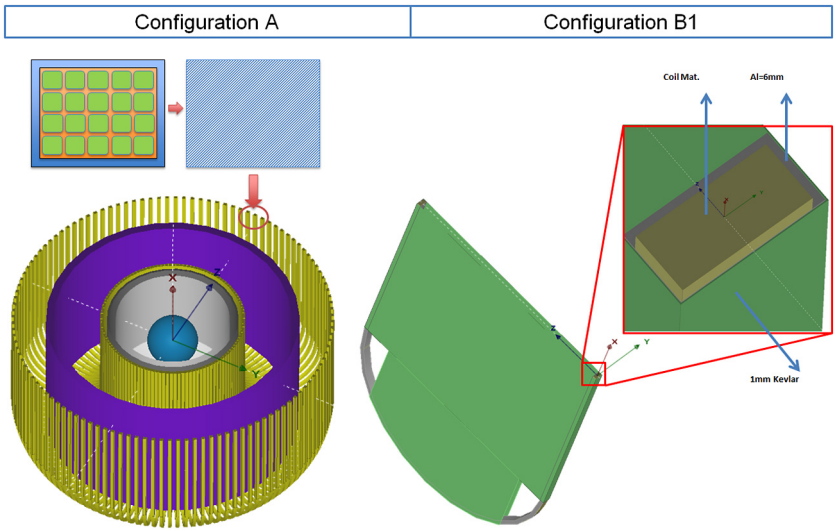

Fig. 7. SR2S geometrical models: details on the structure modeling assumptions (down).

4. Results

In the following paragraphs simulation results are shown and discussed. Fig. 8, Fig. 9 and Table 2 report for all the studied cases the simulation results in terms of sex averaged effective dose, computed using the ICRP123 fluence to dose conversion factors obtained through the ICRP reference human phantom. Since a restricted lateral source was used for the simulations the obtained effective dose for each case is given as a percentage of the dose that an astronaut would get if in deep space without any shielding (this situation is referred as the "free space" case) and not in terms of absolute effective dose in Sv. Results are initially given separating the contribution to the effective dose of GCR ions with atomic number $Z \leq 2$ (1st row of Fig. 8) from the one of GCR ions with $Z > 3$ (2nd row of Fig. 8), given the different behavior of the two groups. Then the two contributions are summed up in Fig. 9.

Values referred to the Columbus habitat are obtained with both magnetic field off and on. In the latter case this means that the active shielding system model is not present in the simulation.

4.1. Configuration A

When analyzing the parametric analysis it is evident the impact to the effective dose of the secondary particles (in particular neutrons) generated by the fragmentation of high-energy particles and their nuclear reactions with the structural materials, is described in a first approximation by the Bradt–Peters equation (Eq. (6)) (Durante and Cucinotta, 2011; Calvelli, 2013) for which the probability of fragmentation (cross-section σ) is:

$$\sigma = \pi r_0^2 c_1(E)\left(A_P^{1/3} + A_T^{1/3} - c_2(E)\right)^2 \quad (6)$$

where r_0 is the nucleon radius (approximately 1.3 fm), c_1 and c_2 are semi-empirical terms, A_P and A_T the projectile and target atomic mass numbers. In order to diminish the production of the secondary particles, it follows from (6) that the active shielding structure around the habitat should be designed with materials having the atomic weight A_T as low as possible.

The first row of Fig. 8 shows that the Effective Dose for protons and alpha particles initially increases when increasing the structure mass varying the material density till 50%, corresponding to a structure of about 150 tons. Such an effect is due to the secondary particle production. For densities greater than 50% the *stopping power* of the structures materials prevails on the secondary production and Effective Dose decreases reaching a value close to the one found in *free space*. The 100% density value corresponds to about 315 tons of materials and about 100 g/cm^2 of areic mass. When instead the magnetic field is off, doses substantially behave with the same trends but have greater absolute values.

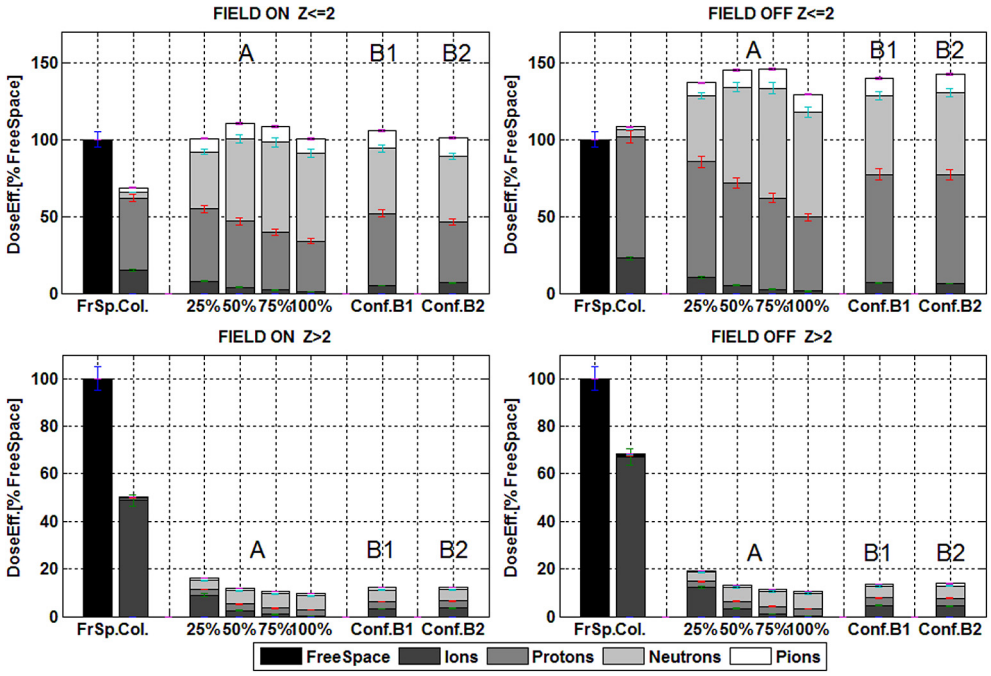

Fig. 8. Monte Carlo simulations results for the configurations A and B. $Z \leq 2$ in the first row and $Z > 2$ in the second row.

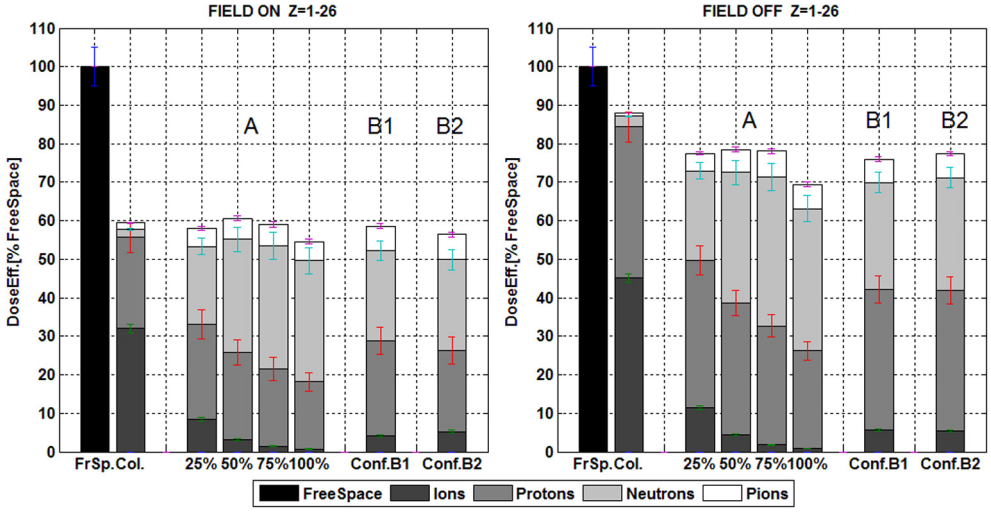

Fig. 9. Monte Carlo simulations results for the configurations A and B for $Z = 1$–26.

Table 2
Sex averaged effective dose [as a percentage of the free space dose, i.e. Effective Dose in deep space without shielding] resulting from the Monte Carlo simulations results for the configurations A and B.

Conf. type	Field 0 Tm	Field 7.9 Tm	Field 11.9 Tm
Columbus	88.0% ± 4.72%	59% ± 4%	–
Conf. A 25%	77.5% ± 4.19%	58% ± 2%	–
Conf. A 50%	78.5% ± 2.36%	61% ± 2%	–
Conf. A 75%	78.1% ± 1.93%	59% ± 1%	–
Conf. A 100%	69.4% ± 1.41%	55% ± 1%	–
Conf. B1	76.0% ± 0.90%	59% ± 1%	–
Conf. B2	77.4% ± 0.81%	–	56% ± 1%

Simulations show that the Effective Dose delivered by the HZE ions ($Z = 3$ to 26) is not evidently influenced by the magnetic field presence when realistic values of mass are considered (see Fig. 8, 2nd row); this can be explained by the low range values for the majority of HZE at the energies considered in the simulations, namely less than 25 g cm^{-2}. Even for the case where only the Columbus module is surrounded by a magnetic field, its mass is contributing in a major way into stopping the incoming ions. Increasing the structure mass, doses are then reduced to small values and the majority of HZE ions are stopped. As expected, for these primary particles the passive shielding contribution prevails, however as the structure thickness increases (for density values greater than 50%), the effective dose is reduced in a slower way. This is due to the secondary particles produced by the HZE ions interactions with matter, which continue their path in the volumes reaching greater depths.

Fig. 9 shows the values of the total Effective Dose considering the contribution of both light ions ($Z = 1$ and 2) and heavy ions ($Z = 3$ to 26).

Considering configuration A, with 100% of mass, the total lateral effective dose is reduced by a factor of about 2. It should be recalled that this value is obtained considering only a fictitious lateral source, addressing the problem of dealing with the endcaps to

the second part of the study (Fig. 5) and with the goal to compare the efficiencies of different toroidal solutions.

4.2. Configuration B

The results for the B1 and B2 configurations are shown in Fig. 7 next to the previous ones obtained in the parametric analysis. The total effective dose, for the field "on" case, is about 58.7% (B1 – 7.9 Tm) and 56.5% (B2 – 11.9 Tm) of "*free space*" dose, values comparable to what obtained for Configuration A with the 25% of the total density (i.e. about 80 tons) which was 58.1% of "free space" dose. This means that Configuration B1 (104 tons) is quite equivalent to Configuration A (25% density, 80 tons) from a radiation shielding point of view, keeping the same magnetic bending power of 7.9 Tm. Configuration B2 reduces the effective dose of about 2.2% with respect to the B1 case but in spite of an increase of the bending power of about 50%, from 7.9 to 11.9 Tm.

It is to notice how the differences in doses between the "field on" and "field off" cases for all the configurations (A – 100% of density, B1 and B2) is ranging from about 14.7% of "the free space" effective dose for the configuration A, to 17.3% for B1 and to 20.9% for B2 (for a total dose reduction of 43.5%). Therefore, it was possible to increase the field effectiveness by choosing materials that optimize the radiation shielding, pointing out how it is necessary to combine passive and active shielding trying to reach the optimum synergy between them.

Therefore, given the fact that configurations B1 and B2 use lower atomic mass number materials with respect to configuration A, their total weight is less than configuration A, for a comparable radiation protection. It is also important to note that while configuration B1 and B2 were designed taking into account the mechanical strength requirements resulting from an assessment on the arising magnetic forces, being therefore potentially achievable in a real case, for configuration A – 25% (25% of the total density) an adequate stress analysis was not performed but values of densities were virtually changed to obtain a better understanding of the mass impact on the physical mechanisms determining the active shielding performances.

5. Conclusions

The future human exploration of the Solar System depends on many technological challenges. Cosmic rays are one of the main showstoppers and the SR2S project aims to assess the feasibility of a space radiation superconducting magnetic shield.

The performed analyses with Monte Carlo simulations on the other hand showed for the first time that in a realistic situation the secondary particles, produced by the interaction of cosmic rays with the active shielding materials, are the major source of the crew radiation dose. Moreover a large part of the secondary particles are fast neutrons that cannot be deflected by the magnetic field, therefore their production drastically reduces the effectiveness of the active shield.

The first attempt to deal with this issue was to decrease the total structure mass and to optimize the material choice, resulting in the design of configuration B1. The second attempt (configuration B2) consisted of increasing the shielding power to 11.9 Tm. In both cases the resulting effective dose reduction of the active shield was not significantly improved compared to the "no-field" case with the same mass, reaching about 20% for configuration B2. Additional simulations have been started modifying structural materials to study the impact on neutron production, and they will the subject of a dedicated publication.

An effort to reduce the amount of material is necessary too. In this sense, further developments in the framework of the SR2S project will concern new configurations to achieve better dose reductions. Open configurations which take advantage by a wide stray field were analyzed but resulted inefficient: they require huge magnetic structures to generate an effective shielding field. Other solutions are possible, including non-axial toroidal geometries, and will be investigated. Furthermore, once identified the most promising active configuration, the efficiency of the magnetic field will be analyzed performing a comparison with an optimized passive shield, having the same mass per unit area.

These results represent the estimated overall dose reduction based on the physics model (Agostinelli et al., 2003) available today, that could suffers of all epistemic uncertainties described previously. For future study a reduction of the extrapolation energy range for the adopted physics models, depending on the availability of the data, will be desirable.

Acknowledgements

This work is supported by Thales Alenia Space Italia, INFN and co-funded by the EU FP7 SR2S Project.

The SR2S consortium is funded by the EU 7th Framework Programme (FP7, Grant agreement for collaborative project No. 313224) in the context of the call title SPA 2012 2.2.02, key technology for in-space activities. The participants are the Italian Institute for Nuclear Physics (INFN), which coordinates the project, Thales Alenia Space Italia (Turin), CGS (Milan), Columbus Superconductors (Genoa), CEA (Saclay), CERN and Carr Communications (Dublin).

The authors wish to thank Dr. E. Tracino, Prof. Dr. M. Durante and Dr. Maria Grazia Pia for the fruitful discussions and helpful suggestions.

References

Agostinelli, S., Alison, J., Amako, K., et al., 2003. Geant4 – a simulation toolkit. Nucl. Instrum. Methods A 506, 250–303.

Battiston, R., et al., 2013. Superconducting magnets for astroparticle shielding in interplanetary manned missions. IEEE Trans. Appl. Supercond. 23 (3).

Braun, W.V., 1969. Will mighty magnets protect voyagers to planets. Popular Science (January), 98–100.

Calvelli, V., 2013. Studio di un sistema di toroidi superconduttori per applicazioni spaziali. Thesis. Università degli Studi di Genova.

Chytracek, R., McCormick, J., Pokorski, W., Santin, G., 2006. Geometry description markup language for physics simulation and analysis applications. IEEE Trans. Nucl. Sci. 53 (5 Part 2), 2892–2896.

Cucinotta, F., 2013. How safe is safe enough? Radiation risk for a human mission to Mars. PLoS ONE 8 (10), 1.

Durante, M., Cucinotta, F.A., 2011. Physical basis of radiation protection in space travel. Rev. Mod. Phys. 83, 1245–1281.

ECSS Space Environment Standard (ECSS E-10-04), 2008.

Hoffman, J.A., Fisher, P., Batischev, O., 2005. Use of superconducting magnet technology for astronaut radiation protection. NIAC Phase I, Final Rep. Contract CP 04-01. NASA Inst. Adv. Concepts (NIAC), Washington, DC, USA.

ICRP, 2013. Assessment of radiation exposure of astronauts in space. ICRP Publication 123. Ann. ICRP 42 (4).

Ivantchenko, A.V., Ivanchenko, V.N., Molina, J.-M.Q., Incerti, S.L., 2012. Geant4 hadronic physics for space radiation environment. Int. J. Radiat. Biol. 88 (1–2), 171–175.

Musenich, R., et al., 2014. A magnesium diboride superconducting toroid for astroparticle shielding. IEEE Trans. Appl. Supercond. 24 (3).

Santin, G., et al., 2005. GRAS: a general-purpose 3-D modular simulation tool for space environment effects analysis. IEEE Trans. Nucl. Sci. 52 (6), 2294–2299.

Spillantini, P., 2011. Superconducting magnets and mission strategies for protection from ionizing radiation in interplanetary manned missions and interplanetary habitats. Acta Astron. 68 (3/4), 1430–1439.

Townsend, L.W., Wilson, J.W., Shinn, J.L., Nealy, J.E., Simonsen, L.C., 1990. Radiation protection effectiveness of a proposed magnetic shielding concept for manned Mars missions. SAE Technical Paper No. 901343. In: 20th Intersociety Conference on Environmental Systems. Williamsburg, VA, July 9–2, 1990.

Wilson, J.W., Miller, J., Konradi, A., Cucinotta, F.A., 1997. Shielding strategies for human space exploration. NASA CP 3360. Johnson Space Center, Langley Res. Center, Houston, TX, USA.

Zeitlin, C., et al., 2013. Science 340, 1080–1084.